DFTT 06/2006
hep-ph/0604273

Pseudo-observables in Axial gauge

E. Accomando

Dipartimento di Fisica Teorica, Università di Torino,
and INFN, Sezione di Torino,
Via P. Giuria 1, 10125 Torino, Italy

Abstract:
We have given a first application of the Axial gauge à la Dams and Kleiss to the Standard Model (SM) physics at the LHC. We have focused on the issue of providing a well-behaved signal definition in presence of potentially strong gauge cancellations at high energies. As a first illustration, we have analysed the production of WZ vector-boson pairs, which gives rise to four final-state fermions. Purely leptonic final states, pp $\to l\bar{\nu}_l l'\bar{l}'$, have been numerically investigated in the region of high center-of-mass energies and large scattering angles, particularly sensitive to gauge dependences. We have found that the Axial gauge is the appropriate framework to recover a meaningful separation of signal and irreducible background over the full energy domain.

April 2006

1 Introduction

This letter deals with the phenomenology of the SM electroweak interactions at high energy scales. The high energy region has an enormous potential for particle discovery. A large set of new signatures is expected in this kinematical domain at the upcoming and future colliders. Of course, the signals might be very complicated and the background overwhelming, expecially in hadronic environments.

With increasing the energy, new channels with many particles in the final state will indeed open up, making difficult to understand the underlying physics. In this intricate context, the comparison between measurements and theoretical predictions will be far from easy task. A long chain of Monte Carlo simulations will be employed to deconvolute the observed quantities back to the partonic variables. With this prospect, identifying the signal configuration and picking out the kinematical regions where it is expected to be enhanced over the background could probe decisive in the data analysis.

In this letter, the question we want to address is precisely how to disentagle the signal from its irreducible background. Commonly, what we consider as a signal is represented by a subset of Feynman diagrams which describes the particles we are searching for as intermediate states. In most of the cases, this sub-contribution is not separately gauge invariant. The signal may indeed contain gauge-invariance-breaking terms which are only cancelled against their irreducible-background counterpart in the total amplitude.

In principle, any bare selection of signal is not theoretically well-defined; only gauge-independent quantities can be related to physical observables. However, questions of principles are often of scarce practical relevance. The point is to evaluate the numerical impact of the potentially badly-behaving terms. The answer is influenced by different factors. It varies according to the process at hand, the energy scale the reaction occurs at, and the gauge-fixing choice.

It is quite a known fact that at LEP2 energies the gauge-invariance-breaking terms are generally unimportant, when computed in the 't Hooft Feynman gauge. But, they might cause strong gauge cancellations between the various Feynman diagrams contributing to a given process at higher energy scales. This phenomenon is more and more enhanced as the off-shellness of the intermediate-state particles and the number of graphs increase [1, 2, 3]. Complex processes with many particles in the final state might thus undergo huge interferences, making it senseless any signal selection.

In this letter we show that considering the Standard Model in the Axial gauge à la Dams and Kleiss [4] allows one to recover a quasi-gauge-invariant signal definition. In order to discuss this issue, we focus on the production of WZ gauge-boson pairs with large invariant mass M_{WZ} at the upcoming Large Hadron Collider (LHC), giving rise to four-fermion final states. The signal definition for this kind of processes has a well established reference. It has been in fact stated and largely used at LEP2 for the analysis of WW and ZZ physics.

The interest in the WZ process is not only in giving a typical example of high energy electroweak phenomenology. The LHC will in fact collect thousands of di-boson events [5], hence giving prospects for a detailed investigation of the WWZ trilinear couplings in this channel. Possible anomalous self-interactions, which parametrize deviations from SM predictions due to new physics occurring at TeV scales, are indeed expected to increasingly

enhance the gauge-boson pair-production cross section at large di-boson invariant masses. Extracting the signal is thus of vital importance to measure the involved trilinear gauge coupling.

The paper is organized as follows: in Sect. 2 we briefly describe the axial gauge. The general setup of our numerical analysis is given in Sect. 3. In Sect. 4, we discuss the possibility of a well-behaved signal definition, comparing the results in Unitary and Axial gauge. Our findings are summarized in Sect. 5. The SM Feynman rules in the axial gauge are listed in Appendix A.

2 Axial gauge

One of the most appealing reasons for computing SM processes in the Axial gauge is that it can provide a more severe check on gauge invariance (see for instance Ref. [6]). In the following sections, we point out a further advantage, namely the possibility to minimize the gauge cancellations between Feynman diagrams at high energies. Here, we simply give a brief description of the Axial gauge content.

The formalism is not exceedingly cumbersome. There are indeed unphysical bosonic particles, as intermediate states, but no Fadeev-Popov ghosts. Moreover, two realizations are possible. The first one keeps the bilinear terms in the unphysical bosons and the W or Z particles, giving rise to mixed propagators [7]. The latter has diagonalized propagators, but new interaction vertices [4]. In the following, we discuss and use this latter approach.

The Axial gauge manifests its nature in the gauge-fixing part of the lagrangian

$$Ł_{\text{gauge-fixing}} = -\tfrac{1}{2}\lambda n^\mu A^a_\mu A^a_\nu n^\nu - \tfrac{1}{2}\lambda (n\cdot B)^2, \tag{2.1}$$

where A^a_μ (a=1,2,3) are the SU(2) gauge fields, and B_μ belongs to U(1). The four-vector n_μ represents the gauge invariance control parameter, the physical observables must be independent of. The resulting Feynman rules, obtained in the limit $\lambda \to \infty$, are summarized in Appendix A.

Once rewritten A^3 and B in terms of the physical fields Z and γ, and parametrizing the Higgs-doublet field as

$$\phi = \frac{1}{\sqrt{2}}\begin{pmatrix} \sqrt{2}\phi_{\rm W} \\ v + {\rm H} + i\phi_{\rm Z} \end{pmatrix}, \qquad v = 2\sqrt{-\mu^2/\lambda_\phi} \tag{2.2}$$

where H represents the Higgs field with mass $\rm M_H$ and λ_ϕ the Higgs self-coupling, the mixing terms between physical and unphysical neutral fields are

$$\begin{aligned} Ł_{\rm Z\phi Z,bilinear} = &-\tfrac{1}{2}(\partial^\nu {\rm Z}^\mu)(\partial_\nu {\rm Z}_\mu) + \tfrac{1}{2}(\partial^\mu {\rm Z}_\mu)(\partial^\nu {\rm Z}_\nu) + \tfrac{1}{2}{\rm M}_{\rm Z}^2 {\rm Z}_\mu {\rm Z}^\mu \\ &- \tfrac{1}{2}\lambda n^\mu {\rm Z}_\mu {\rm Z}_\nu n^\nu + \tfrac{1}{2}(\partial^\mu \phi_{\rm Z})(\partial_\mu \phi_{\rm Z}) - {\rm M}_{\rm Z}{\rm Z}^\mu \partial_\mu \phi_{\rm Z}. \end{aligned} \tag{2.3}$$

This part of the Lagrangian can be diagonalized in momentum space by applying the following transformation

$$\phi_{\rm Z}(k) \to \phi_{\rm Z}(k) + 2i{\rm M}_{\rm Z}\frac{k^\mu {\rm Z}_\mu(k)}{k^2}. \tag{2.4}$$

After the diagonalization, the quadratic terms in the Lagrangian for the field Z give rise to the Z-boson propagator

$$\Delta_{\nu\mu} = \frac{-i\left(g_{\nu\mu} - \frac{n_\nu k_\mu + n_\mu k_\nu}{n\cdot k} + k_\nu k_\mu \frac{n^2 + (k^2 - \mathrm{M}_\mathrm{Z}^2)/\lambda}{(n\cdot k)^2}\right)}{k^2 - \mathrm{M}_\mathrm{Z}^2 + i\epsilon}. \tag{2.5}$$

Taking the limit $\lambda \to \infty$, one recovers the expression reported in Appendix A.1. An analogous procedure applies to the W-boson, and gives back the same propagator with $\mathrm{M_Z}$ replaced by $\mathrm{M_W}$.

The boson propagators in axial gauge display the peculiar property of being well-behaved at high energy. In the unitary gauge, the term $k_\mu k_\nu/\mathrm{M}_V^2$ ($V = \mathrm{W}, \mathrm{Z}$) appearing in the numerator of the propagator leads to gauge-invariance-breaking terms of order s/M_V^2 (with s the center-of-mass energy squared) in individual Feynman diagrams. By contrast, in axial gauge each numerator factor k_μ is suppressed by a corresponding factor $1/(k\cdot n)$, preventing the growth with energy of individual diagrams and the subsequent appearence of strong gauge cancellations between them. This important property, shared also by the new vertices, and its phenomenological consequences are the focus of this letter.

3 Setup of the numerical analysis

We consider the class of processes $\mathrm{pp} \to l\bar{\nu}_l l'\bar{l}'$, where $l, l' = \mathrm{e}$ or μ. In our notation, $l\bar{\nu}_l$ indicates both $l^-\bar{\nu}_l$ and $l^+\nu_l$. These processes are characterized by three isolated charged leptons plus missing energy in the final state. They include WZ production as intermediate state.

Since the two incoming hadrons are protons and we sum over final states with opposite charges, we find

$$\begin{aligned}\mathrm{d}\sigma^{h_1h_2}(P_1,P_2,p_f) = \int_0^1 \mathrm{d}x_1\mathrm{d}x_2 \sum_{U=u,c}\sum_{D=d,s}\Big[&f_{\bar{\mathrm{D}},\mathrm{p}}(x_1,Q^2) f_{\mathrm{U},\mathrm{p}}(x_2,Q^2)\,\mathrm{d}\hat{\sigma}^{\bar{\mathrm{D}}\mathrm{U}}(x_1P_1,x_2P_2,p_f)\\ &+ f_{\bar{\mathrm{U}},\mathrm{p}}(x_1,Q^2) f_{\mathrm{D},\mathrm{p}}(x_2,Q^2)\,\mathrm{d}\hat{\sigma}^{\bar{\mathrm{U}}\mathrm{D}}(x_1P_1,x_2P_2,p_f)\\ &+ f_{\bar{\mathrm{D}},\mathrm{p}}(x_2,Q^2) f_{\mathrm{U},\mathrm{p}}(x_1,Q^2)\,\mathrm{d}\hat{\sigma}^{\bar{\mathrm{D}}\mathrm{U}}(x_2P_2,x_1P_1,p_f)\\ &+ f_{\bar{\mathrm{U}},\mathrm{p}}(x_2,Q^2) f_{\mathrm{D},\mathrm{p}}(x_1,Q^2)\,\mathrm{d}\hat{\sigma}^{\bar{\mathrm{U}}\mathrm{D}}(x_2P_2,x_1P_1,p_f)\Big]\end{aligned} \tag{3.1}$$

in leading order of QCD.

For the masses we use the input values [8]:

$$M_\mathrm{W} = 80.425\,\mathrm{GeV}, \qquad M_\mathrm{Z} = 91.1876\,\mathrm{GeV}, \qquad m_\mathrm{b} = 4.9\,\mathrm{GeV}. \tag{3.2}$$

All fermions but the b-quark are taken to be massless.

The weak mixing angle is fixed by $s_\mathrm{W}^2 = 1 - M_\mathrm{W}^2/M_\mathrm{Z}^2$. Moreover, we adopted the so called G_μ-scheme, which effectively includes higher-order contributions associated with the running of the electromagnetic coupling and the leading universal two-loop m_t-dependent corrections. This corresponds to parametrize the lowest-order matrix element in terms of the effective coupling $\alpha_{G_\mu} = \sqrt{2}G_\mu M_\mathrm{W}^2 s_\mathrm{W}^2/\pi$.

Additional input parameters are the quark-mixing matrix elements whose values have been taken to be $|V_{\rm ud}| = 0.974$ [9], $|V_{\rm cs}| = |V_{\rm ud}|$, $|V_{\rm us}| = |V_{\rm cd}| = \sqrt{1-|V_{\rm ud}|^2}$, and zero for all other relevant matrix elements.

For the numerical results presented here, we have used the fixed-width scheme with $\Gamma_{\rm Z}$ and $\Gamma_{\rm W}$ from standard formulas

$$\Gamma_{\rm Z} = \frac{\alpha M_{\rm Z}}{24 s_{\rm W}^2 c_{\rm W}^2}\Big[21 - 40 s_{\rm W}^2 + \frac{160}{3} s_{\rm W}^4 + \frac{m_{\rm b}^4}{M_{\rm Z}^4}(24 s_{\rm W}^2 - 16 s_{\rm W}^4) - 9\frac{m_{\rm b}^2}{M_{\rm Z}^2} + \frac{\alpha_s}{\pi}\Big(15 - 28 s_{\rm W}^2 + \frac{88}{3} s_{\rm W}^4\Big)\Big] \tag{3.3}$$

and

$$\Gamma_{\rm W} = \frac{\alpha M_{\rm W}}{2 s_{\rm W}^2}\left[\frac{3}{2} + \frac{\alpha_s}{\pi}\right]. \tag{3.4}$$

For the strong coupling we use $\alpha_s = 0.117$.

As to parton distributions, we have used CTEQ6M [10] at the following factorization scale:

$$Q^2 = \frac{1}{2}\Big(M_{\rm W}^2 + M_{\rm Z}^2 + P_{\rm T}^2(l\bar{\nu}_l) + P_{\rm T}^2(l'\bar{l}')\Big) \tag{3.5}$$

This scale choice appears to be appropriate for the calculation of differential cross sections, in particular for vector-boson transverse-momentum distributions [11, 12].

We have, moreover, implemented a general set of cuts, proper for LHC analyses, defined as follows:

- charged lepton transverse momentum $P_{\rm T}(l) > 20\,{\rm GeV}$,
- missing transverse momentum $P_{\rm T}^{\rm miss} > 20\,{\rm GeV}$,
- charged lepton pseudo-rapidity $|\eta_l| < 3$, where $\eta_l = -\ln(\tan(\theta_l/2))$, and θ_l is the polar angle of particle l with respect to the beam,
- lepton pair invariant mass ${\rm M}(l'\bar{l}') \geq 0.201\,{\rm GeV}$.

These cuts approximately simulate the detector acceptance. For the processes considered, we have also implemented further cuts which are described in due time. In the following sections, we present results for the LHC at CM energy $\sqrt{s} = 14\,{\rm TeV}$ and an integrated luminosity $L = 100\,{\rm fb}^{-1}$.

4 Gauge scheme and signal definition

In this section we discuss how to identify and separate the signal of WZ production from the background. Let us first define these two contributions diagrammatically.

The generic process pp $\to l\bar{\nu}_l l'\bar{l}'$ is described by the Feynman diagrams drawn in Fig. 1. The three doubly-resonant graphs mediated by W and Z-boson production are displayed in the first row. From LEP2 on, this is what we call CC03 signal for the

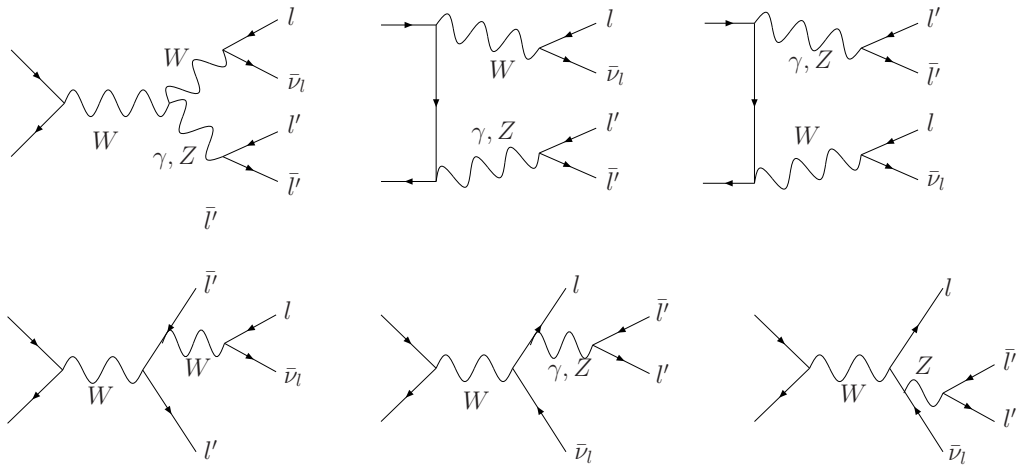

Figure 1: Feynman diagrams for the full process pp $\to l\bar{\nu}_l l'\bar{l}'$. The first row shows the doubly-resonant CC03 diagrams for WZ production (when the photon is neglected). The latter represents the irreducible background, which the photon contribution in the first row must be added to.

di-boson production [1]. The irreducible background, represented by singly-resonant and non-resonant diagrams, is instead shown in the second row, and partially in the first row by the graphs with virtual photon exchange.

From a practical point of view, the aim is to maximize the signal over the background ratio, picking out the kinematical regions where the first one is more enhanced and applying appropriate cuts to suppress the latter. Hence, having at disposal a clear separation among the two contributions is highly desirable.

Unfortunately, signal and background do not individually preserve gauge invariance. Each of them includes indeed gauge-invariance-breaking terms which are only cancelled in their sum. Hence, only the full set of Feynman diagrams, i.e. the complete amplitude, is theoretically well-behaved. Despite of that, one could still define a pseudo-observable using the pure doubly-resonant CC03 contribution.

The possibility of such a definition strongly depends on the size of the terms which violate gauge invariance. As well known, their numerical impact can vary according to the energy and the off-shellness of the intermediate particles in the process. This generally makes their behaviour unpredictable. The off-shellness is indeed a variable one cannot always limit. In the easy case at hand the virtuality of the produced W and Z bosons can be arbitrarily reduced, in this way suppressing the gauge violating terms. In the limit of on-shell WZ production, the CC03 diagrams would in fact constitute a gauge independent set. But there are also opposite examples. When the virtual particles in a process are

[1]The CC03 cross section was introduced and discussed in Refs. [13, 14] in order to extract the WW signal from the full set of $e^+e^- \to 4f$ processes.

exchanged in t-channel, they cannot be forced anymore to be almost on-shell, leaving thus unconstrained the dangerous terms.

In the next two sections, we show that the gauge-fixing choice is the actual control key for the gauge-invariance-breaking terms.

4.1 CC03 in Unitary Gauge

The CC03 cross section was introduced at LEP2 in order to combine the different final state measurements from the various collaborations, and increase the statistics. Usually defined either in the Unitary gauge or in the 't Hooft-Feynman gauge, the CC03 cross section is not an observable, but at LEP2 energies it was taken as a useful quantity. It contains interesting informations about triple gauge boson vertices, and is sensible to the M_W value. At LEP2, the CC03 signal was then classified as a pseudo-observable and widely used. Its reliability was based on its closeness to the full result, which implies neglegible gauge violating terms. But, the crucial caveat was that such a signal definition might become very problematic at future high energy colliders, owing to the much larger backgrounds and gauge dependences.

In Unitary gauge, delicate cancellations between doubly-resonant (DR) and non-DR diagrams characterize the behaviour of off-shell cross sections in the high-energy regime. In the 't Hooft-Feynman gauge, this kind of cancellations generally appear moderately weakened, but still persist. In the massless limit we are working in, the two gauge schemes coincide. In the following, we refer to that as Unitary gauge.

For the example at hand, the behaviour of DR and non-DR diagrams is shown in Fig. 2 (see also Ref. [2]). There, we have plotted the tree-level cross section as a function of the cut on the transverse momentum of the reconstructed Z-boson, $P_T(l'\bar{l}')$. This cut selects large di-boson center-of-mass energies and wide scattering angles of the produced vector-bosons. This is exactly the kinematical region dominated by the longitudinal gauge-boson production, and thus particularly sensitive to the gauge-violation effects we want to analyse.

The first two curves in Fig. 2 represent, from top to bottom, the contribution of the pure doubly-resonant diagrams, and the full result including all Feynman diagrams which contribute to the same final state. The first clear information one can extract from the plot is that the DR contribution ($pp \to WZ \to 4f$), which is lower than the exact result ($pp \to 4f$) by about 1% around threshold, increases with energy relatively to the full result. For $P_T^{cut}(l'\bar{l}') = 300\,\mathrm{GeV}$, the difference between the two cross sections is already of order 20%, and at very large energies the DR diagrams can even overestimate the result by a factor 2 or more.

This behavior can only be explained with the existence of strong interferences between DR and non-DR subsets of diagrams, which are not separately gauge-independent. The consequence is that in Unitary gauge it is extremely hard to consider the pure DR contribution as a pseudo-observable. The diagrammatic approach, commonly adopted at LEP2 for WW and ZZ physics, fails when describing the di-boson production at the LHC in the high-P_T region. In this gauge scheme, the only sensible observable is the total contribution. Thus, any signal definition seems to be completely lost. A method which has been proposed to recover it consists in the double-pole approximation (DPA).

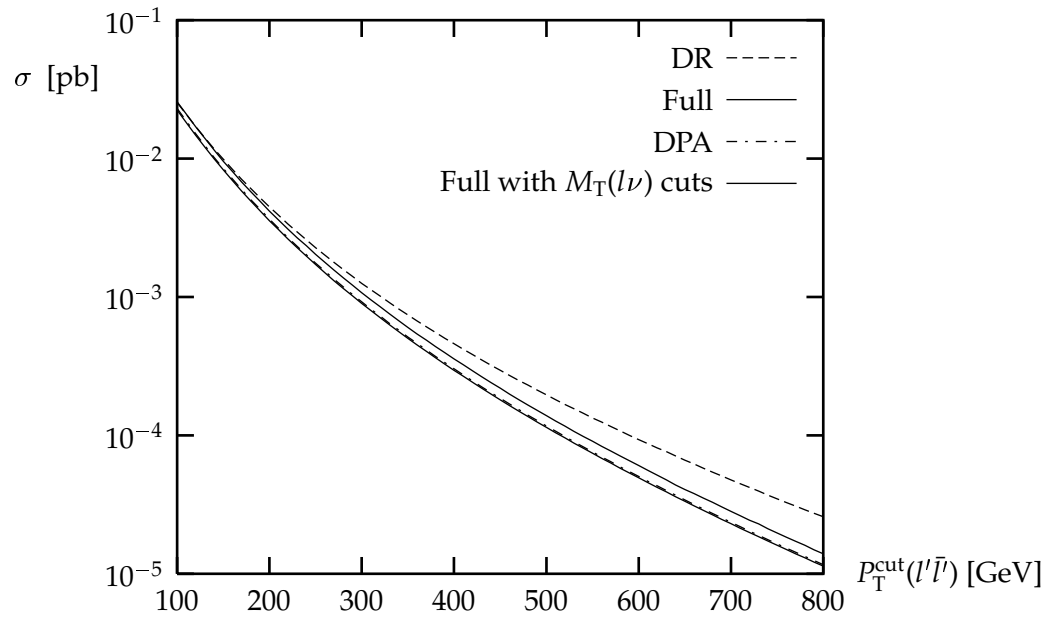

Figure 2: Born cross section for the full process $pp \to l\bar{\nu}_l l'\bar{l}'$ at $\sqrt{s} = 14\,\mathrm{TeV}$ as a function of the cut on the transverse momentum of the reconstructed Z-boson. Standard cuts are applied. Legends as explained in the text.

This approximation emerges from the CC03 diagrams upon projecting the vector-boson momenta in the matrix element to their on-shell values. This means that the DPA is based on the residue of the double resonance, which is related to the sub-processes of on-shell di-boson production and subsequent on-shell vector-boson decay. Owing to that, the DPA shares the property of preserving gauge invariance.

For the case at hand, the DPA cross section is shown in Fig. 2, where it is represented by the third curve from top to bottom. One can see that the DPA is lower than the total cross section, their difference amounting to roughly -15% for $P_{\rm T}(l'\bar{l}')$ cuts above 100 GeV. As displayed by the solid line overlapping the DPA curve, the gap reduces to the per-cent level if one imposes cuts on the masses of the two lepton-pairs: $|\mathrm{M}(l'\bar{l}') - \mathrm{M_Z}| \leq 20\,\mathrm{GeV}$ and $M_{\rm T}(l\bar{\nu}_l) = \sqrt{E_{\rm T}^2(l\bar{\nu}_l) - P_{\rm T}^2(l\bar{\nu}_l)} \leq \mathrm{M_W} + 20\,\mathrm{GeV}$. This shows that, in contrast to the CC03 cross section in Unitary gauge, the DPA is theoretically well defined, and might be considered as a good estimate of the di-boson production when restricted to the doubly-resonant region.

However, the method has two substantial limitations. A first obvious price to be paid is the exclusion of the kinematical regions outside the s-channel resonances, where the DPA is not valid. The second limit is represented by the processes where the intermediate resonant particles are exchanged in t-channel (i.e. they have space-like virtuality). In this case, the DPA cannot be applied. One can rely only on its analogous given by the Equivalent Vector Boson approximation (EVBA), whose reliability is still debated for it crucially depends on the applied kinematical cuts.

The two approximations can give an estimate of the signal. But their goodness must be first checked against an exact computation. This bottom-top procedure of bringing the

easier tool, represented by the approximate signal, to match the full result proves to be extremely powerful in some case. The DPA has been successfully employed for evaluating higher order corrections to the full process. But, also the reverse can be highly useful. That means defining an a-priori signal, which the full result should converge to. This is essential in experiments. A scan of the full phase space in order to see where the signal is more enhanced, and how the background can be suppressed might in fact be decisive for data analyses.

In both Unitary and 't Hooft-Feynman gauge schemes this is not possible. In the next section, we show that the Axial gauge is the appropriate framework to obtain an independent and well-behaved signal definition.

4.2 CC03 in Axial Gauge

We consider the same process as before, pp $\to l\bar{\nu}_l l'\bar{l}'$, in Axial gauge. The matrix element is written according to the Feynman rules written in Appendix A (see also Ref. [4]).

Since we assume all fermions to be massless, the contribution of the unphysical fields $\phi_{\rm Z}$ and $\phi_{\rm W}$ to the amplitude can be ignored. This simplifies the computation sensibly, but does not alter the generality of the results. The cross sections and distributions presented in this section have been obtained using $n_\mu = (2, 1, 1, 1)$ as gauge vector. However, we checked that the non-gauge-invariant quantities we analyse in the following have a very little dependence on that.

Our aim is to show that in Axial gauge the diagrammatic approach can be recovered. This means that a signal, i.e. a selected subset of diagrams, can be considered as a pseudo-observable even if non-gauge-invariant. To this end, we have chosen a phase-space region characterized by large center of mass energies and large scattering angles of the produced vector bosons, $P_{\rm T}(l'\bar{l}') > 800\,{\rm GeV}$. This is in fact the kinematical domain where the gauge-violating terms, if there, would be enhanced as displayed in Fig. 2 for the Unitary gauge.

We have moreover selected four weakly correlated variables which reflect our most direct expectations on the signal and background behaviour, namely:

- M($l'\bar{l}'$) - the invariant mass of the lepton pair which could come from the Z-boson decay,
- M($ll'\bar{l}'$) - the invariant mass of the three charged leptons,
- M($l\bar{\nu}_l\bar{l}'$) - the invariant mass of the two leptons which could come from the W-boson decay plus the opposite-sign lepton coming from the Z-boson,
- cos($l\bar{l}'$) - the cosine of the angle between the charged lepton coming from the W-boson and the opposite-sign lepton from the Z-boson.

The corresponding differential cross sections are plotted in Fig. 3. There, the solid line represents the full contribution coming from all ten tree-level diagrams. The two dashed lines compare instead the CC03 signal in the two gauge schemes. The long-dashed line gives CC03 in Unitary gauge (or t'Hooft-Feynman gauge), while the dashed one shows

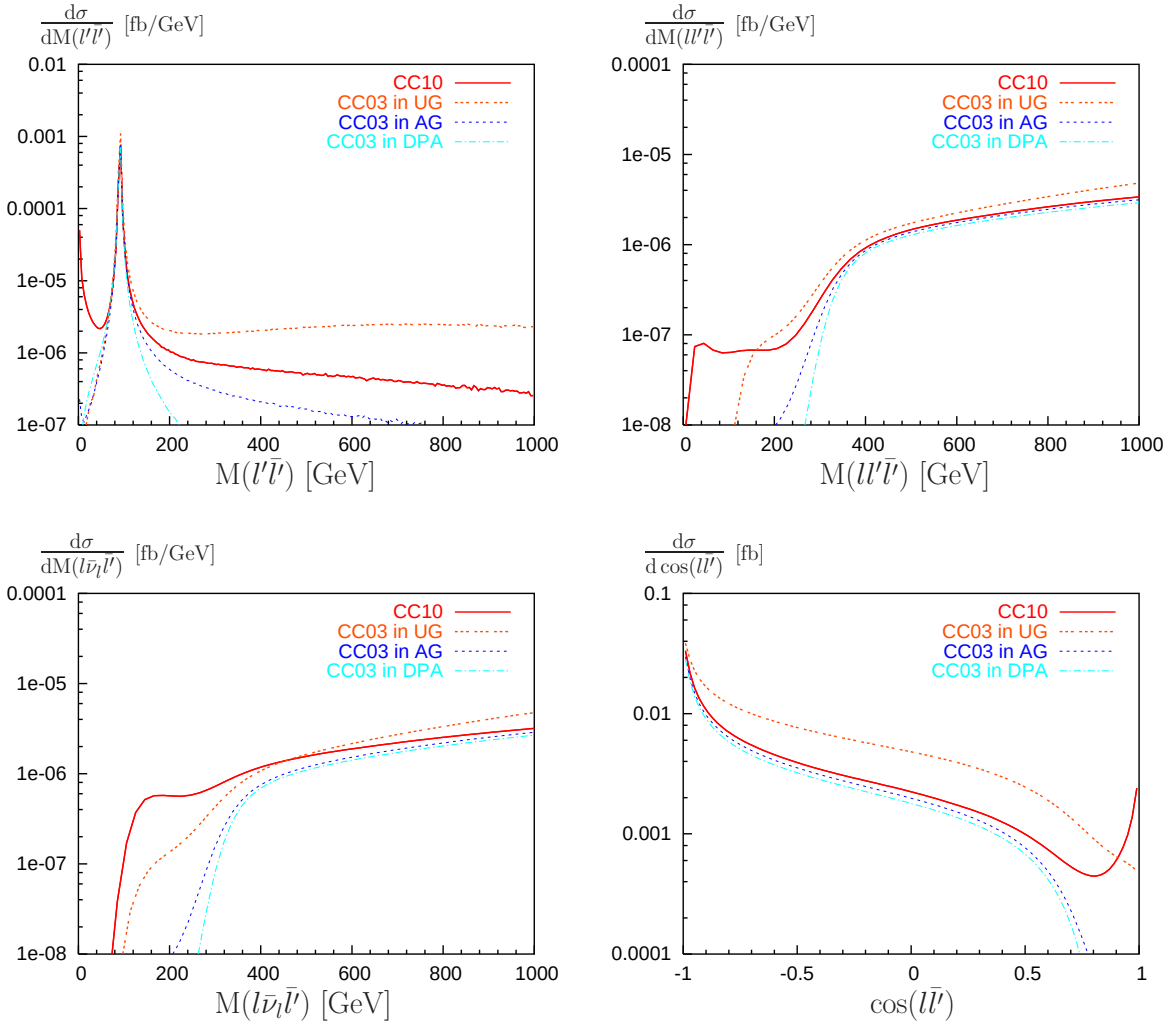

Figure 3: Distributions for WZ production. (a) Invariant mass of the same-flavour charged lepton pair. (b) Invariant mass of the charged leptons. (c) Invariant mass of the lepton pair which might come from a W-boson, and the opposite-charge lepton which might come from a Z-boson. (d) Cosine of the angle between opposite-charge and different-flavour leptons. The contributions of the four final states $l\bar{\nu}_l l'\bar{l}'$ where $l, l' = e, \mu$ are summed up, and standard cuts as well as $P_{\mathrm{T}}(\mathrm{Z}) > 800\,\mathrm{GeV}$ are applied. Legends as explained in the text.

the CC03 signal in Axial gauge. Finally, as a reference, the dot-dashed line displays the DPA result. The first left-side plot contains the $\mathrm{M}(l'\bar{l}')$ invariant mass. This observable peaks on $\mathrm{M_Z}$, receiving the dominant contribution from the CC03 signal. But, it is also expected to have some tail outside the resonant region, owing to all W-singly-resonant and non-resonant diagrams drawn in Fig. 1. In particular, the photon exchange should generate a rise at low invariant mass values. The expected behaviour is well reproduced by the solid line, as it must.

Expectations are equally satisfied if one looks at the CC03 signal in Axial gauge. The so-defined signal is indeed concentrated around the Z-resonance, going sharply to zero

beyond a few Γ_Z. The gauge-invariant DPA result comes as a further confirmation of the well-behaved CC03 in Axial gauge. The gauge-violating terms thus appear under control.

Compared to these results, the Unitary gauge shows its ill-defined nature. In this scheme, the CC03 signal presents a long tail at large invariant masses, which is completely unphysical. It in fact stands up over the full result by an order of magnitude, implying the presence of huge gauge cancellations between the CC03 diagrams and the rest. The Z-boson invariant mass distribution clearly shows that the presence of the gauge-violating terms is strictly linked to the virtuality of the intermediate gauge boson.

An analogous discussion holds for the other two invariant mass distributions plotted in Fig. 3. The top-right-side and the bottom-left-side plots represent the momentum of the fermion propagator in graphs 5 and 4 of Fig. 1, respectively. The two differential cross sections get the dominant contributions from the large masses, as the W and Z bosons are produced back-to-back mainly. But, they have also a sizeable low-mass component coming from the afore-mentioned singly-resonant diagrams, as shown by the solid line. Once again, the CC03 signal in Axial gauge matches the expectations, while the Unitary gauge gives a result which lies above the total differential cross section, and displays unphysical tails.

The last distribution on the bottom-right-side shows the cosine of the angle between the two charged leptons which could come from the W and the Z bosons. The CC03 signal in Axial gauge peaks in the backward direction, as the W and Z bosons are produced back-to-back. The full CC10 shows in addition a forward rise coming from the graphs 4 and 5 in Fig. 1. These contributions are in fact enhanced when the two leptons are produced collinearly. The Unitary gauge shows once more the usual effect. It distorts and overestimates both the signal and the total differential cross sections, as for the previous variables.

5 Conclusions

In this letter, we have applied for the first time the Axial gauge à la Dams and Kleiss to analyze the SM physics at the LHC. For a precise understanding of the high-energy phenomenology, having at hand an unambiguous separation of signal and background is mandatory. We have shown that the Axial gauge is the appropriate framework to obtain a quasi-gauge-invariant signal definition. It allows in fact to isolate the signal trasparently, keeping the gauge-violating terms well under control even at very high energy scales.

For this first application, we have chosen to analyse the well-stated WZ production process (a more complicated process mediated by vector boson scattering will be discussed in Ref. [15]). The signal definition has in this case a very well known reference, namely the CC03 (NC02) cross section which was introduced and widely used at LEP2 for WW (ZZ) physics. This quantity is not gauge invariant. It contains gauge-violating terms which cancel only when summed up with the irreducible-background counterpart. Nevertheless, it can be taken as a useful pseudo-observable if the gauge dependence is kept well below the experimental accuracy.

That was the case at LEP2 energies, where the gauge-violating-breaking terms were probed to be generally unimportant when computed in the 't Hooft-Feynman gauge.

With increasing the energy, the size of the potentially badly-behaving terms might grow dramatically. Strong gauge cancellations between the various diagrams contributing to the same final state can take place, making any signal selection senseless.

We have shown that the Axial gauge can recover the diagrammatic approach, and give a well-behaved signal definition over the full energy domain.

Acknowledgements

G. Passarino is gratefully acknowledged for valuable comments on the subject treated and for carefully reading the manuscript. This work was supported by the Italian Ministero dell'Istruzione, dell'Università e della Ricerca (MIUR) under contract Decreto MIUR 26-01-2001 N.13 "Incentivazione alla mobilità di studiosi stranieri ed italiani residenti all'estero".

Appendix

A Feynman rules

In this appendix, we list the SM Feynman rules in Axial gauge. We adopt the same conventions as in Ref. [4], which are here below summarized:

1. The Feynman rules that involve fermions are written only for the first generation of leptons $(\mathrm{e}, \nu_{\mathrm{e}})$.

2. Particles and anti-particles are represented by lines with an arrow. The momentum flows in the direction of the arrow. For particles described by lines without arrow, the momentum flows towards the vertex.

3. We use the following notation:

$$\mathrm{g_w} = \frac{\mathrm{g_e}}{\sin\theta_{\mathrm{w}}}; \quad \mathrm{g_z} = \frac{\mathrm{g_e}}{\sin\theta_{\mathrm{w}}\cos\theta_{\mathrm{w}}}; \quad p_l = \frac{1}{2}(1-\gamma^5); \quad p_r = \frac{1}{2}(1+\gamma^5).$$

4. If reversing all arrows on a vertex yields a different vertex, that vertex is also a vertex of the theory. The corresponding vertex factor is obtained by conjugation of the original vertex, except for one factor of i, and by reversing the sign of all momenta that belong to particles that do not carry an arrow on their line. In the following, we give the expression of only one sample vertex (the paired one must be derived).

A.1 Propagators

$\underline{\qquad}_{\mathrm{B}(k)}$ $\qquad \dfrac{-i\left(g_{\nu\mu} - \frac{n_\nu k_\mu + n_\mu k_\nu}{n\cdot k} + k_\nu k_\mu \frac{n^2}{(n\cdot k)^2}\right)}{k^2 + i\epsilon}$

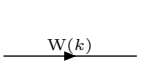

$$\frac{-i\left(g_{\nu\mu}-\frac{n_\nu k_\mu+n_\mu k_\nu}{n\cdot k}+k_\nu k_\mu\frac{n^2}{(n\cdot k)^2}\right)}{k^2-\mathrm{M}_\mathrm{W}^2+i\epsilon}$$

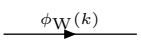

$$\frac{i}{k^2}$$

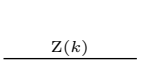

$$\frac{-i\left(g_{\nu\mu}-\frac{n_\nu k_\mu+n_\mu k_\nu}{n\cdot k}+k_\nu k_\mu\frac{n^2}{(n\cdot k)^2}\right)}{k^2-\mathrm{M}_\mathrm{Z}^2+i\epsilon}$$

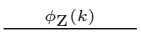

$$\frac{i}{k^2}$$

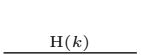

$$\frac{i}{k^2-\mathrm{M}_\mathrm{H}^2+i\epsilon}$$

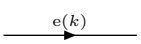

$$\frac{i(\not{k}+\mathrm{m_e})}{k^2-\mathrm{m}_\mathrm{e}^2+i\epsilon}$$

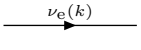

$$\frac{i(\not{k}+\mathrm{m}_{\nu_\mathrm{e}})}{k^2-\mathrm{m}_{\nu_\mathrm{e}}^2+i\epsilon}$$

A.2 Triple boson couplings without Higgs

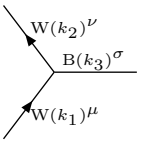

$$i\mathrm{g_e}\Big[\,g^{\nu\sigma}(k_2^\mu+k_3^\mu)+g^{\mu\sigma}(k_1^\nu-k_3^\nu)-g^{\mu\nu}(k_1^\sigma+k_2^\sigma) -\mathrm{M}_\mathrm{W}^2\left(g^{\nu\sigma}\frac{k_1^\mu}{k_1^2}+g^{\mu\sigma}\frac{k_2^\nu}{k_2^2}-(k_1^\sigma+k_2^\sigma)\frac{k_1^\mu}{k_1^2}\frac{k_2^\nu}{k_2^2}\right)\Big]$$

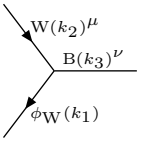

$$i\mathrm{g_e}\mathrm{M_W}\left(g^{\mu\nu}-\frac{(k_1^\nu+k_2^\nu)k_2^\mu}{k_2^2}\right)$$

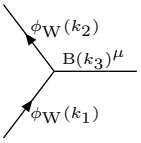

$$i\mathrm{g_e}(k_1^\mu+k_2^\mu)$$

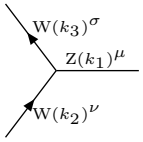

$$
\begin{aligned}
& i\mathrm{g_w}\cos\theta_\mathrm{w}\Big[-g^{\nu\sigma}(k_2^\mu+k_3^\mu)-g^{\mu\nu}(k_1^\sigma-k_2^\sigma)+g^{\mu\sigma}(k_1^\nu+k_3^\nu) \\
& \quad +\mathrm{M_Z^2}\sin^2\theta_\mathrm{w}\left(g^{\mu\sigma}\frac{k_2^\nu}{k_2^2}+g^{\mu\nu}\frac{k_3^\sigma}{k_3^2}\right) \\
& \quad +\frac{1}{2}\mathrm{M_Z^2}\left(-(k_1^\sigma-k_2^\sigma)\frac{k_1^\mu}{k_1^2}\frac{k_2^\nu}{k_2^2}-(k_1^\nu+k_3^\nu)\frac{k_1^\mu}{k_1^2}\frac{k_3^\sigma}{k_3^2}\right) \\
& \quad +\mathrm{M_Z^2}\left(\frac{1}{2}-\sin^2\theta_\mathrm{w}\right)(k_2^\mu+k_3^\mu)\frac{k_2^\nu}{k_2^2}\frac{k_3^\sigma}{k_3^2}\Big]
\end{aligned}
$$

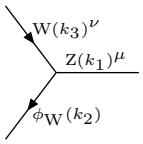

$$
-i\mathrm{g_z}\mathrm{M_W}\left(\sin^2\theta_\mathrm{w}g^{\mu\nu}-\frac{1}{2}\frac{(k_1^\nu+k_2^\nu)k_1^\mu}{k_1^2}+\left(\cos^2\theta_\mathrm{w}-\frac{1}{2}\right)\frac{(k_2^\mu+k_3^\mu)k_3^\nu}{k_3^2}\right)
$$

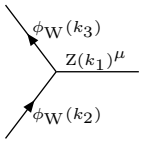

$$
i\mathrm{g_w}\,(k_2^\mu+k_3^\mu)\left(\cos\theta_\mathrm{w}-\frac{1}{2\cos\theta_\mathrm{w}}\right)
$$

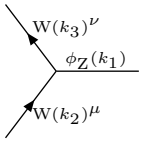

$$
\frac{1}{2}\mathrm{g_w}\mathrm{M_W}\left(\frac{(k_2^\nu-k_1^\nu)k_2^\mu}{k_2^2}-\frac{(k_1^\mu+k_3^\mu)k_3^\nu}{k_3^2}\right)
$$

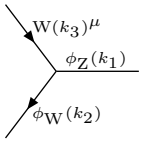

$$
\frac{1}{2}\mathrm{g_w}\,(k_1^\mu+k_2^\mu)
$$

A.3 Triple boson couplings with Higgs

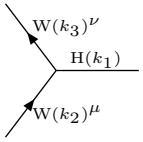

$$
\frac{i}{2}\mathrm{g_w}\mathrm{M_W}\left(2g^{\mu\nu}-\frac{k_3^\nu(k_1^\mu+k_3^\mu)}{k_3^2}+\frac{k_2^\mu(k_1^\nu-k_2^\nu)}{k_2^2}-\mathrm{M_H^2}\frac{k_2^\mu}{k_2^2}\frac{k_3^\nu}{k_3^2}\right)
$$

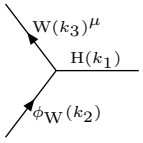

$$
\frac{i}{2}\mathrm{g_w}\left(k_2^\mu-k_1^\mu+\frac{\mathrm{M_H^2}}{k_3^2}k_3^\mu\right)
$$

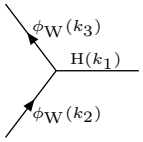

$$
-\frac{i}{2}\mathrm{g_w}\frac{\mathrm{M_H^2}}{\mathrm{M_W}}
$$

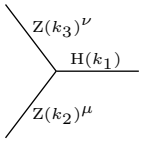

$$
i\mathrm{g_z}\mathrm{M_Z}\left(g^{\mu\nu}+\frac{1}{2}(k_1^\nu-k_2^\nu)\frac{k_2^\mu}{k_2^2}+\frac{1}{2}(k_1^\mu-k_3^\mu)\frac{k_3^\nu}{k_3^2}+\frac{1}{2}\mathrm{M_H^2}\frac{k_2^\mu}{k_2^2}\frac{k_3^\nu}{k_3^2}\right)
$$

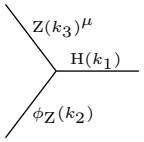

$$\frac{1}{2}\mathrm{g_z}\left(k_1^\mu - k_2^\mu + \mathrm{M_H^2}\frac{k_3^\mu}{k_3^2}\right)$$

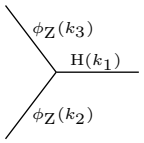

$$-\frac{i}{2}\mathrm{g_z}\frac{\mathrm{M_H^2}}{\mathrm{M_Z}}$$

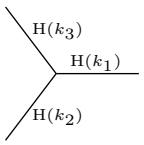

$$-\frac{3i}{2}\mathrm{g_w}\frac{\mathrm{M_H^2}}{\mathrm{M_W}}$$

A.4 Couplings to the Fermions

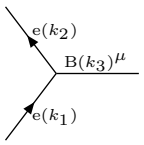

$$i\mathrm{g_e}\gamma^\mu$$

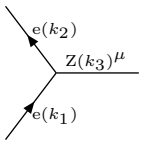

$$i\mathrm{g_z}\left(\frac{1}{2}\gamma^\mu p_l - \gamma^\mu \sin^2\theta_\mathrm{w} + \frac{1}{2}\frac{\mathrm{m_e}}{k_3^2}k_3^\mu\gamma^5\right)$$

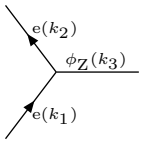

$$\frac{1}{2}\mathrm{g_z}\frac{\mathrm{m_e}}{\mathrm{M_Z}}\gamma^5$$

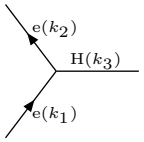

$$-\frac{i}{2}\mathrm{g_w}\frac{\mathrm{m_e}}{\mathrm{M_W}}$$

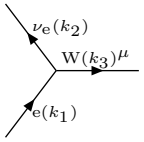

$$-\frac{i\mathrm{g_w}}{\sqrt{2}}V_{11}\left(\gamma^\mu p_l + \left(\mathrm{m}_{\nu_\mathrm{e}}p_l - \mathrm{m_e}p_r\right)\frac{k_3^\mu}{k_3^2}\right)$$

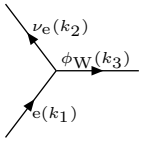

$$\frac{i}{\sqrt{2}}\frac{\mathrm{g_w}}{\mathrm{M_W}}V_{11}\left(\mathrm{m}_{\nu_\mathrm{e}}p_l - \mathrm{m_e}p_r\right)$$

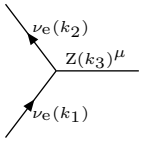

$$-\frac{i}{2}\mathrm{g_z}\left(\gamma^\mu p_l + \mathrm{m}_{\nu_\mathrm{e}}\gamma^5\frac{k_3^\mu}{k_3^2}\right)$$

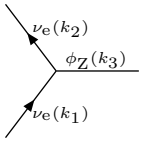

$$-\frac{1}{2}\mathrm{g_w}\frac{\mathrm{m}_{\nu_\mathrm{e}}}{\mathrm{M_W}}\gamma^5$$

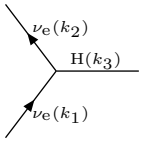

$$-\frac{i}{2}\mathrm{g_w}\frac{\mathrm{m}_{\nu_\mathrm{e}}}{\mathrm{M_W}}$$

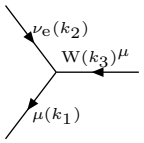

$$-\frac{i\mathrm{g_w}}{\sqrt{2}}V_{21}^\dagger\left(\gamma^\mu p_l-\left(\mathrm{m}_\mu p_l-\mathrm{m}_{\nu_\mathrm{e}}p_r\right)\frac{k_3^\mu}{k_3^2}\right)$$

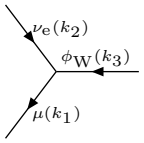

$$-\frac{i}{\sqrt{2}}\frac{\mathrm{g_w}}{\mathrm{M_W}}V_{21}^\dagger\left(\mathrm{m}_\mu p_l-\mathrm{m}_{\nu_\mathrm{e}}p_r\right)$$

A.5 Quadruple boson couplings among B, W and $\phi_{\rm W}$

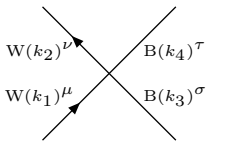

$$i\mathrm{g_e^2}\left(-2g^{\mu\nu}g^{\sigma\tau}+g^{\mu\sigma}g^{\nu\tau}+g^{\mu\tau}g^{\nu\sigma}+2\mathrm{M_W^2}g^{\sigma\tau}\frac{k_1^\mu}{k_1^2}\frac{k_2^\nu}{k_2^2}\right)$$

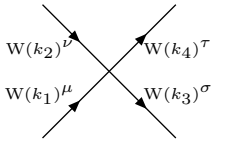

$$\begin{aligned}i\mathrm{g_w^2}\Big[\,&2g^{\mu\nu}g^{\sigma\tau}-g^{\mu\sigma}g^{\nu\tau}-g^{\mu\tau}g^{\nu\sigma}\\&+\frac{1}{2}\mathrm{M_W^2}\left(g^{\nu\tau}\frac{k_1^\mu}{k_1^2}\frac{k_3^\sigma}{k_3^2}+g^{\nu\sigma}\frac{k_1^\mu}{k_1^2}\frac{k_4^\tau}{k_4^2}+g^{\mu\tau}\frac{k_2^\nu}{k_2^2}\frac{k_3^\sigma}{k_3^2}+g^{\mu\sigma}\frac{k_2^\nu}{k_2^2}\frac{k_4^\tau}{k_4^2}\right)\\&-\frac{1}{2}\mathrm{M_W^2M_H^2}\frac{k_1^\mu}{k_1^2}\frac{k_2^\nu}{k_2^2}\frac{k_3^\sigma}{k_3^2}\frac{k_4^\tau}{k_4^2}\Big]\end{aligned}$$

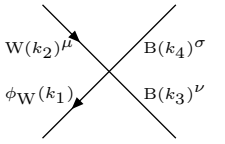

$$-2i\mathrm{g_e^2M_W}g^{\nu\sigma}\frac{k_2^\mu}{k_2^2}$$

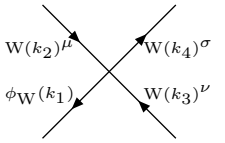

$$\frac{i}{2}\mathrm{g_w^2M_W}\left(-g^{\nu\sigma}\frac{k_2^\mu}{k_2^2}-g^{\mu\sigma}\frac{k_3^\nu}{k_3^2}+\mathrm{M_H^2}\frac{k_2^\mu}{k_2^2}\frac{k_3^\nu}{k_3^2}\frac{k_4^\sigma}{k_4^2}\right)$$

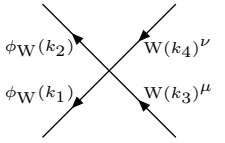

$$-\frac{i}{2}\mathrm{g_w^2M_H^2}\frac{k_3^\mu}{k_3^2}\frac{k_4^\nu}{k_4^2}$$

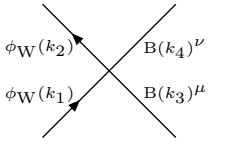

$$2i\mathrm{g_e^2}g^{\mu\nu}$$

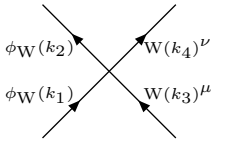

$$\frac{i}{2}\mathrm{g_w^2}\left(g^{\mu\nu}-\mathrm{M_H^2}\frac{k_3^\mu}{k_3^2}\frac{k_4^\nu}{k_4^2}\right)$$

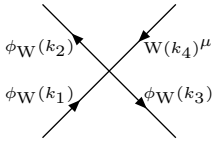

$$\frac{i}{2}\mathrm{g_w^2}\frac{\mathrm{M_H^2}}{\mathrm{M_W}}\frac{k_4^\mu}{k_4^2}$$

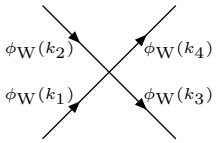

$$-\frac{i}{2}\mathrm{g_w^2}\frac{\mathrm{M_H^2}}{\mathrm{M_W^2}}$$

A.6 Quadruple boson couplings with Z, and without $\phi_{\rm Z}$ or H

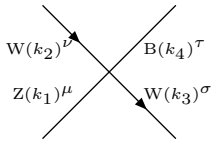

$$i\mathrm{g_e g_w}\cos\theta_{\rm w}\left[-2g^{\mu\tau}g^{\nu\sigma}+g^{\mu\nu}g^{\sigma\tau}+g^{\mu\sigma}g^{\nu\tau}+\mathrm{M_Z^2}\left(\frac{1}{2}g^{\sigma\tau}\frac{k_1^\mu}{k_1^2}\frac{k_2^\nu}{k_2^2}-\frac{1}{2}g^{\nu\tau}\frac{k_1^\mu}{k_1^2}\frac{k_3^\sigma}{k_3^2}+g^{\mu\tau}(2\cos\theta_w^2-1)\frac{k_2^\nu}{k_2^2}\frac{k_3^\sigma}{k_3^2}\right)\right]$$

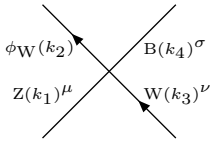

$$i\mathrm{g_e g_z M_W}\left(\frac{1}{2}g^{\nu\sigma}\frac{k_1^\mu}{k_1^2}+g^{\mu\sigma}(1-2\cos^2\theta_{\rm w})\frac{k_3^\nu}{k_3^2}\right)$$

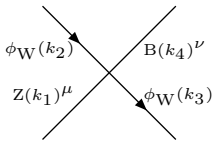

$$i\mathrm{g_e g_z}(2\cos^2\theta_{\rm w}-1)g^{\mu\nu}$$

$$-i\mathrm{g_w^2}\Big[\ \cos^2\theta_{\rm w}\left(2g^{\mu\nu}g^{\sigma\tau}-g^{\mu\sigma}g^{\nu\tau}-g^{\mu\tau}g^{\nu\sigma}\right)$$

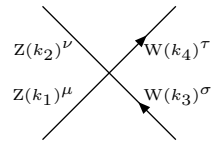

$$+\frac{1}{2}\mathrm{M_Z^2}\sin^2\theta_{\rm w}\left(\frac{1}{\sin^2\theta_{\rm w}}g^{\sigma\tau}\frac{k_1^\mu}{k_1^2}\frac{k_2^\nu}{k_2^2}+g^{\nu\tau}\frac{k_1^\mu}{k_1^2}\frac{k_3^\sigma}{k_3^2}-g^{\nu\sigma}\frac{k_1^\mu}{k_1^2}\frac{k_4^\tau}{k_4^2}+g^{\mu\tau}\frac{k_2^\nu}{k_2^2}\frac{k_3^\sigma}{k_3^2}-g^{\mu\sigma}\frac{k_2^\nu}{k_2^2}\frac{k_4^\tau}{k_4^2}+\left(4\cos^2\theta_{\rm w}-\frac{1}{\sin^2\theta_{\rm w}}\right)g^{\mu\nu}\frac{k_3^\sigma}{k_3^2}\frac{k_4^\tau}{k_4^2}-\frac{\mathrm{M_H^2}}{2\sin^2\theta_{\rm w}}\frac{k_1^\mu}{k_1^2}\frac{k_2^\nu}{k_2^2}\frac{k_3^\sigma}{k_3^2}\frac{k_4^\tau}{k_4^2}\right)\Big]$$

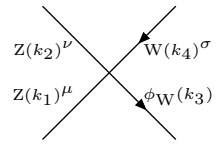

$$-\frac{i}{2}\frac{\mathrm{g_e^2 M_W}}{\cos^2\theta_{\rm w}}\left[\ g^{\nu\sigma}\frac{k_1^\mu}{k_1^2}+g^{\mu\sigma}\frac{k_2^\nu}{k_2^2}+\left(\frac{1}{\sin^2\theta_{\rm w}}-4\cos^2\theta_{\rm w}\right)g^{\mu\nu}\frac{k_4^\sigma}{k_4^2}+\frac{1}{2\sin^2\theta_{\rm w}}\mathrm{M_H^2}\frac{k_1^\mu}{k_1^2}\frac{k_2^\nu}{k_2^2}\frac{k_4^\sigma}{k_4^2}\right]$$

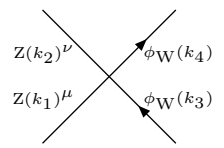

$$i\mathrm{g_z^2}\left(\left(\frac{1}{2}-2\cos^2\theta_{\rm w}\sin^2\theta_{\rm w}\right)g^{\mu\nu}+\frac{1}{4}\mathrm{M_H^2}\frac{k_1^\mu}{k_1^2}\frac{k_2^\nu}{k_2^2}\right)$$

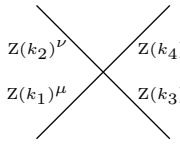

$$-\frac{i}{2}\mathrm{g_z^2 M_Z^2}\Big(\, g^{\mu\nu}\frac{k_3^\sigma}{k_3^2}\frac{k_4^\tau}{k_4^2} + g^{\mu\sigma}\frac{k_2^\nu}{k_2^2}\frac{k_4^\tau}{k_4^2} + g^{\mu\tau}\frac{k_2^\nu}{k_2^2}\frac{k_3^\sigma}{k_3^2} + g^{\nu\sigma}\frac{k_1^\mu}{k_1^2}\frac{k_4^\tau}{k_4^2} + g^{\nu\tau}\frac{k_1^\mu}{k_1^2}\frac{k_3^\sigma}{k_3^2} + g^{\sigma\tau}\frac{k_1^\mu}{k_1^2}\frac{k_2^\nu}{k_2^2} + \frac{3}{2}\mathrm{M_H^2}\frac{k_1^\mu}{k_1^2}\frac{k_2^\nu}{k_2^2}\frac{k_3^\sigma}{k_3^2}\frac{k_4^\tau}{k_4^2}\Big)$$

A.7 Quadruple boson couplings with one ϕ_Z and no H

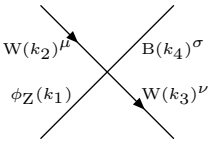

$$\frac{1}{2}\mathrm{g_e g_w M_W}\left(g^{\nu\sigma}\frac{k_2^\mu}{k_2^2} - g^{\mu\sigma}\frac{k_3^\nu}{k_3^2}\right)$$

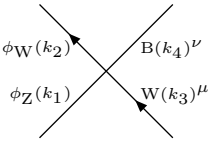

$$\frac{1}{2}\mathrm{g_e g_w}g^{\mu\nu}$$

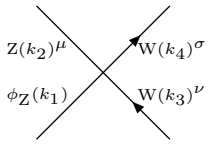

$$\frac{1}{2}\mathrm{g_e^2 M_Z}\left(-\frac{g^{\nu\sigma}}{\sin^2\theta_w}\frac{k_2^\mu}{k_2^2} - g^{\mu\sigma}\frac{k_3^\nu}{k_3^2} + g^{\mu\nu}\frac{k_4^\sigma}{k_4^2} + \frac{1}{2}\frac{\mathrm{M_H^2}}{\sin^2\theta_\mathrm{w}}\frac{k_2^\mu}{k_2^2}\frac{k_3^\nu}{k_3^2}\frac{k_4^\sigma}{k_4^2}\right)$$

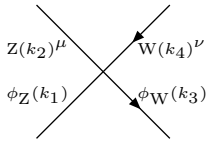

$$-\mathrm{g_e^2}\left(\frac{1}{2\cos\theta_\mathrm{w}}g^{\mu\nu} + \frac{\mathrm{M_H^2}}{4\sin^2\theta_\mathrm{w}\cos\theta_\mathrm{w}}\frac{k_2^\mu}{k_2^2}\frac{k_4^\nu}{k_4^2}\right)$$

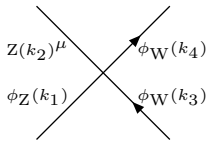

$$\frac{1}{4}\mathrm{g_z^2}\frac{\mathrm{M_H^2}}{\mathrm{M_Z}}\frac{k_2^\mu}{k_2^2}$$

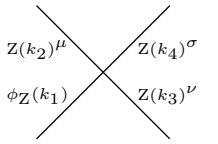

$$-\frac{1}{2}\mathrm{g_z^2 M_Z}\left(g^{\nu\sigma}\frac{k_2^\mu}{k_2^2} + g^{\mu\sigma}\frac{k_3^\nu}{k_3^2} + g^{\mu\nu}\frac{k_4^\sigma}{k_4^2} + \frac{3}{2}\mathrm{M_H^2}\frac{k_2^\mu}{k_2^2}\frac{k_3^\nu}{k_3^2}\frac{k_4^\sigma}{k_4^2}\right)$$

A.8 Quadruple boson couplings with multiple ϕ_Z and no H

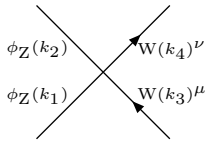

$$i\mathrm{g_w^2}\left(\frac{1}{2}g^{\mu\nu} - \frac{1}{4}\mathrm{M_H^2}\frac{k_3^\mu}{k_3^2}\frac{k_4^\nu}{k_4^2}\right)$$

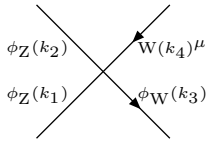

$$\frac{i}{4}\mathrm{g_w^2}\frac{\mathrm{M_H^2}}{\mathrm{M_W}}\frac{k_4^\mu}{k_4^2}$$

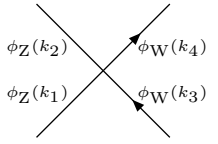

$$-\frac{i}{4}\mathrm{g_w^2}\frac{\mathrm{M_H^2}}{\mathrm{M_W^2}}$$

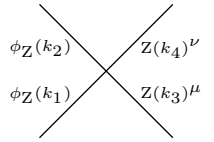

$$\frac{i}{2}\mathrm{g_z^2}\left(g^{\mu\nu}+\frac{3}{2}\mathrm{M_H^2}\frac{k_3^{\mu}}{k_3^2}\frac{k_4^{\nu}}{k_4^2}\right)$$

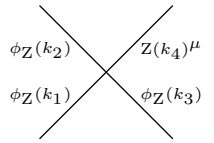

$$\frac{3}{4}\mathrm{g_z^2}\frac{\mathrm{M_H^2}}{\mathrm{M_Z}}\frac{k_4^{\mu}}{k_4^2}$$

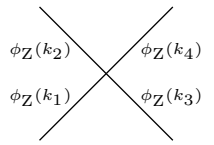

$$-\frac{3}{4}i\mathrm{g_z^2}\frac{\mathrm{M_H^2}}{\mathrm{M_Z^2}}$$

A.9 Quadruple boson couplings with one H

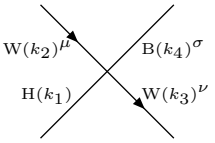

$$-\frac{i}{2}\mathrm{g_e g_w M_W}\left(g^{\nu\sigma}\frac{k_2^{\mu}}{k_2^2}+g^{\mu\sigma}\frac{k_3^{\nu}}{k_3^2}\right)$$

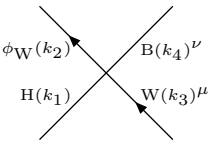

$$\frac{i}{2}\mathrm{g_e g_w}g^{\mu\nu}$$

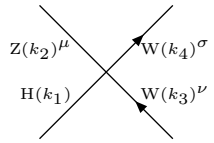

$$\frac{i}{2}\mathrm{g_e^2 M_Z}\left(g^{\mu\sigma}\frac{k_3^{\nu}}{k_3^2}+g^{\mu\nu}\frac{k_4^{\sigma}}{k_4^2}\right)$$

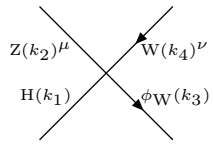

$$-\frac{i}{2}\frac{\mathrm{g_e^2}}{\cos\theta_{\mathrm{w}}}g^{\mu\nu}$$

A.10 Quadruple boson couplings with multiple H

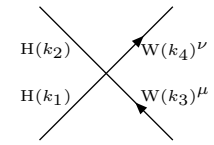

$$i\mathrm{g_w^2}\left(\frac{1}{2}g^{\mu\nu}-\frac{1}{4}\mathrm{M_H^2}\frac{k_3^{\mu}}{k_3^2}\frac{k_4^{\nu}}{k_4^2}\right)$$

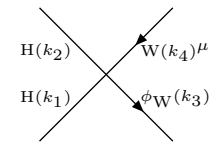

$$\frac{i}{4}\mathrm{g_w^2}\frac{\mathrm{M_H^2}}{\mathrm{M_W}}\frac{k_4^{\mu}}{k_4^2}$$

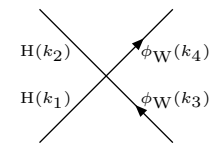

$$-\frac{i}{4}\mathrm{g_w^2}\frac{\mathrm{M_H^2}}{\mathrm{M_W^2}}$$

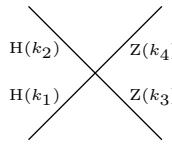

$$\frac{i}{2}\mathrm{g_z^2}\left(g^{\mu\nu}+\frac{1}{2}\mathrm{M_H^2}\frac{k_3^\mu}{k_3^2}\frac{k_4^\nu}{k_4^2}\right)$$

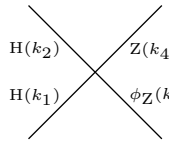

$$\frac{1}{4}\mathrm{g_z^2}\frac{\mathrm{M_H^2}}{\mathrm{M_Z}}\frac{k_4^\mu}{k_4^2}$$

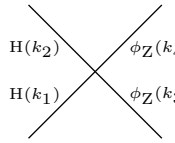

$$-\frac{i}{4}\mathrm{g_w^2}\frac{\mathrm{M_H^2}}{\mathrm{M_W^2}}$$

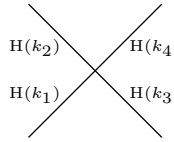

$$-\frac{3}{4}i\mathrm{g_w^2}\frac{\mathrm{M_H^2}}{\mathrm{M_W^2}}$$

References

[1] R. Kleiss and J. W. Stirling, Phys. Lett. B **182** (1986) 75.

[2] Elena Accomando, Ansgar Denner, Stefano Pozzorini, Phys. Rev. D **65** (2002) 073003 [hep-ph/0110114].

[3] E. Accomando, A. Ballestrero, E. Maina, Nucl. Instrum. Meth. A **534** (2004) 265 [hep-ph/0404236]; E. Accomando, A. Ballestrero, A. Belhouari, E. Maina, hep-ph/0505225.

[4] C. Dams and R. Kleiss, Eur. Phys. J. C **34** (2004) 419 [hep-ph/0401136].

[5] S. Haywood, P. R. Hobson, W. Hollik, Z. Kunszt *et al.*, hep-ph/0003275, in *Standard Model Physics (and more) at the LHC*, eds. G. Altarelli and M. L. Mangano, (CERN-2000-004, Genève, 2000) p. 117.

[6] Chris Dams and Ronald Kleiss, Eur. Phys. J. C **36** (2004) 177 [hep-ph/0309336].

[7] Zoltan Kunszt, Davison E. Soper, Nucl. Phys. B **296** (1988) 253.

[8] K. Hagiwara *et al.* [Particle Data Group Collaboration], Phys. Rev. D **66** (2001) 010001.

[9] A. Höcker, H. Lacker, S. Laplace, F. Le Diberder, Eur. Phys. J. C **21** (2001) 225 [hep-ph/0104062].

[10] J. Pumplin, D. R. Stump, J. Huston, H. L. Lai, P. Nadolsky and W. K. Tung, JHEP 0207 (2002) 012 [hep-ph/0201195].

[11] L. Dixon, Z. Kunszt and A. Signer, Phys. Rev. D **60** (1999) 114037 [hep-ph/9907305].

[12] S. Frixione, P. Nason and G. Ridolfi, Nucl. Phys. B **383** (1992) 3.

[13] W. Beenakker *et al.*, in *Physics at LEP2*, eds. G. Altarelli, T. Sjöstrand and F. Zwirner (CERN 96-01, Genève, 1996), Vol.1, p.79 [hep-ph/9602351].

[14] Martin W. Grünewald *et al.*, in *Reports of the working groups on precision calculation for LEP2 physics*, eds. S. Jadach, G. Passarino and R. Pittau (CERN-2000-09-A, Genève, 2000), p. 1 [hep-ph/0005309].

[15] E. Accomando, in preparation.